A True Elliptic-Function Filter Using Triple-Mode Degenerate Cavities

WAI-CHEUNG TANG, MEMBER, IEEE, AND SUJEET K. CHAUDHURI, MEMBER, IEEE

Abstract—A six-pole triple-mode filter capable of a true elliptic-function response has been synthesized and experimentally realized. This was achieved by using a new intercavity iris structure that can control three intercavity-mode couplings simultaneously.

I. Introduction

HIGH-CAPACITY communication satellite transponders usually require many receive and transmit channelizing filters. These channelizing filters went through a series of advancements between 1968 and 1974. In 1969, Comsat Laboratories began an active search for a structure which would enable real transmission zeros to be generated. The geometry which realized this objective was a dual-mode waveguide filter first introduced in 1970 [1] and generalized in 1972 [2]. To realize the frequency selectivity of the INTELSAT IV channelizing filter, the dual-mode filter required only eight poles or four physical cavities. Consequently, weight and volume savings were achieved.

Between 1974 and 1982, the communication satellite industries started to use the dual-mode waveguide filters extensively. However, not much advancement has been made during this period to further improve the multimode waveguide filter structures. In this paper, multimode concepts have been utilized to design a triple-mode waveguide filter (six poles–two cavities) which is capable of realizing true elliptic response. This waveguide structure will allow a further reduction of size and weight in communication satellite waveguide channelizing filters.

Design of multimode filters, using degenerate modes with an identical natural frequency in a single cavity, was first suggested by Lin [3]. In 1969, the first multimode cavity filter, a longitudinal dual-mode waveguide filter, was patented [4]. This filter used two orthogonal TE_{011} modes in a rectangular cavity or TE_{111} modes in a cylindrical cavity. Coupling between electrical cavities was achieved by using the direct-coupling method [5]. Although this dual-mode filter represented a major advancement in filter design, it is not capable of realizing a true elliptic response for filters higher than fourth-order [6]. In 1971, canonical dual-mode structures that enabled the realization of any even-order elliptic-function response in a dual-mode configuration was presented [6]. In the same publication, the use of two orthogonal TE_{111} modes and a TM_{010} mode to construct a sixth-order two-cavity elliptic filter was demonstrated. However, the measured results indicated that they were unable to control all the intercavity couplings simultaneously, and, therefore, failed to achieve a true elliptic function response.

In the case of two-cavity triple-mode filters, one requires three intercavity couplings between six electrical cavities. The coupling mechanism is provided by placing a metal plate with slots (iris) between the two cavities. However, the iris can only provide a two-dimensional independence for intercavity couplings. Therefore, in order to construct a two-cavity six-pole elliptic filter, one must first find an iris structure that can control three intercavity couplings simultaneously.

In this paper, a new iris structure that is capable of providing three independent intercavity couplings is presented in Section III, and it is preceded by the relevant design details of a triple-mode elliptic-function filter in Section II. The experimental performance of a sixth-order triple-mode filter using this new coupling iris is presented in Section IV.

II. Triple-Mode Elliptic-Function Filters

A. Degenerate Cavity Modes

At microwave frequencies, a filter resonator can be constructed by using perfectly conducting walls to enclose a cavity of rectangular, cylindrical, spherical, or any other simple shape. Inside this single-cavity resonator, orthogonality exists among an infinite number of modes. In order to cascade these independent resonator modes to form a filter network, coupling between certain orthogonal modes is required. To produce these couplings, perturbations in the otherwise ideal geometry is used. In order to optimize the coupling efficiency or minimize the perturbation, the modes to be used in a single physical cavity must possess the same resonant frequency or, in other words, they should be degenerate modes.

For a cylindrical cavity resonator of length L and diameter D and bounded by perfectly conducting walls, the resonant wavelength is given by

$$\lambda_0 = 2/\left[2X_{lm}/\pi D)^2 + (n/L)^2\right]^{1/2} \qquad (1)$$

where l, m, and n are integers, and X_{lm} is the mth root of either the Bessel function $J_l(x) = 0$ (for TM modes), or its derivative with respect to the argument (x), $J_l'(x) = 0$ (for

Manuscript received January 3, 1984; revised June 4, 1984.

W.-C. Tang is with Com Dev. Ltd., Cambridge, Ont., Canada.
S. K. Chaudhuri is with the Department of Electrical Engineering, University of Waterloo, Waterloo, Ont., Canada.

0018-9480/84/1100-1449$01.00 ©1984 IEEE

TE mode). Rearranging (1)

$$(Dn/L)^2 = 4(Df)^2/C^2 - (2X_{lm}/\pi)^2, \qquad C = 3\times 10^8 \text{ m/s}. \quad (2)$$

Now, by plotting $(Df)^2$ against $(D/L)^2$ for different modes (X_{lm}), one can see that, at a point where $D/L = 1$, the TE_{111} and TM_{010} are degenerate modes. Furthermore, the two orthogonal TE_{111} and the TM_{010} mode's electric fields are mutually perpendicular to each other. This arrangement is ideal for independent control of the tuning of these three modes.

With TE_{111} and TM_{010} as the degenerate dominant propagation modes, cavity dimensions are determined by using (1) as follows:

For the TM_{010} case

$$D = \lambda_0/1.306 \quad (3)$$

and for the TE_{111} case

$$L = \lambda_0 D/\left[4D^2 - 1.374\lambda_0^2\right]^{1/2}. \quad (4)$$

where λ_0 is the free-space wavelength corresponding to the degenerate resonance frequency f_0.

Intermode coupling between any two modes inside a cavity is achieved by placing a coupling screw at 45° to the electric-field directions of the two modes under consideration, but perpendicular to the third mode. Furthermore, this triple-mode structure, like a dual-mode structure, can provide nonadjacent cavity coupling for realization of finite transmission zeroes. Using two triple-mode cavities, one can synthesize either a six-pole elliptic or six-pole quasi-elliptic function filter.

B. Six-Pole Elliptic Function Synthesis

Filters exhibiting equiripple pass and stopbands which are derived from elliptic integrals are referred to as elliptic filters. The transfer function of an elliptic filter (class B) has the following form:

$$H(s)H^*(s) = 1/\left[1+\epsilon^2 K(s)K(-s)\right]$$

with

$$K(s) = \frac{(a_1^2+s^2)(a_2^2+s^2)\cdots(a_n^2+s^2)}{(b_{n-1}^2+s^2)(b_{n-2}^2+s^2)\cdots(b_1^2+s^2)}$$

where a_i are the locations of transmissions poles, and b_i are the locations of transmission zeros. For a six-pole class-B elliptic-function filter, the above representation for $K(s)$ can be simplified to the following equation:

$$K(s) = \frac{(a_1^2+s^2)(a_2^2+s^2)(a_3^2+s^2)}{(b_2^2+s^2)(b_1^2+s^2)} \quad (5)$$

with the given $H(s)$ a low-pass prototype can be characterized by using the C, K parameter synthesis procedure [7]. In the present case, this prototype network can, in turn, be represented by a coupling matrix and by the corresponding routing diagram, as shown in Fig. 1(a) and (b), respectively. Note that, if a filter has only sequential coupling, a Chebyshev filter will result. In a waveguide elliptic filter, it is the "cross coupling" that provides the mechanism to realize the transmission zeros (b_2, b_1) [1], [8]. Details of these cross couplings in a two-cavity triple-mode filter and the resulting intercavity aperture structure is presented in the next section.

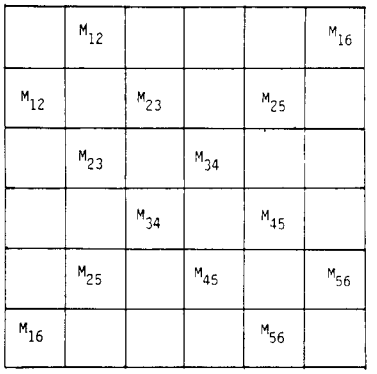

Fig. 1. (a) Coupling matrix for a six-pole elliptic-function filter, and (b) corresponding routing diagram.

III. Intercavity Aperture Design

In the current filter design, electrical cavities 1, 2, and 3 are excited in the physical cavity-1, and the electrical cavities 4, 5, and 6 are excited in the physical cavity-2. Electrical cavities 1, 3, 4, and 6 were chosen to be TE_{111} modes (1 and 6 orthogonal to 3 and 4), and cavities 2 and 5 were taken to be TM_{010} modes. (This choice of cavity-mode sequencing avoids some problems encountered in [6]). To achieve true elliptic-function response, the required coupling matrix for the prototype network is as shown in Fig. 1(a). In this coupling matrix, elements M_{16}, M_{25}, and M_{34} involve energy coupling between two physical cavities, and, therefore, each has to be realized with an appropriate intercavity aperture. Since M_{16} and M_{34} provide coupling between TE_{111} modes, they are usually achieved by placing an iris or a cross at the center of the intercavity aperture (see Fig. 2(a)). From the analysis of the mode pattern of TE_{111} mode fields, it can be seen that these couplings are obtained through the magnetic fields at the slot opening. On the other hand, the element M_{25}, which represents the coupling between the TM_{010} modes in two physical cavities, is achieved with both the magnetic and the axial electric fields at the aperture opening. Thus, in Fig. 2(a), once the lengths of the slots (L_1 and L_2) are fixed to give proper susceptances corresponding to M_{16} and M_{34}, the susceptance providing the coupling between the TM_{010} modes cannot be controlled (width of the slots has to be small compared to the wavelength). In fact, since the axial electric field of TM_{010} is maximum at the center, the

structure of Fig. 2(a) inherently yields a large value for M_{25}, whereas for a true elliptic-function realization, a typical value of M_{25} is quite small. It has been observed that the coupling M_{25} determines the inner transmission zeros (nearest to the passband) and M_{16} gives the outer transmission zeros. Thus, if a proper value for M_{25} is not obtained, a true elliptic-function response cannot be realized.

From the above observations, one can see that, in order to reduce the M_{25} coupling, one must reduce the electric-field coupling of the TM_{010} modes. This can be achieved by moving the coupling slots away from the center of the coupling wall. Based on this logic, a new iris structure is proposed, as illustrated in Fig. 2(b). This aperture structure can satisfy all three (M_{16}, M_{25}, and M_{34}) coupling requirements simultaneously, since it provides two independent sets of parameters, namely, (R(R_1 and R_2) and L(L_1 and L_2) for controlling the intercavity mode couplings. Due to the difference in field patterns of TE_{111} and TM_{010} modes, it is possible to find a combination of R_1, R_2, L_1, and L_2 which satisfies all three coupling values simultaneously.

Based on the work of Matthaei *et al.* [9] and Kudsia [10], the following approximate relationships between the coupling coefficients C (C_{TM} and C_{TE} for TM and TE fields, respectively) and the physical dimensions of the coupling slots (as a function of magnetic and/or electric polarizability) can be derived [11]

$$C_{TM} = \frac{\omega^2\epsilon_0 f_0}{J_1^2(X_{01})\pi k_0^4 l a^2 \Delta f}\left[\frac{Pk_0^4}{\omega^2\epsilon_0}J_0^2\left(\frac{X_{01}\rho}{a}\right) + \mu_0 M\frac{X_{01}^2}{a^2}J_1\left(\frac{X_{01}\rho}{a}\right)\right] \quad (6)$$

$$C_{TE} = \frac{\mu_0 M\beta^2(1.841)^2}{(0.281)a^2k_0^2Z_0^2\epsilon_0\pi l}\cdot\frac{f_0}{\Delta f}J_1'^2\left(\frac{X_{11}'\rho}{a}\right) \quad (7)$$

where

- a radius of the cavity,
- l length of the cavity,
- ρ distance from the center of the aperture to the center of the cavity,
- f_0 center frequency of the filter,
- Δf filter bandwidth,
- M magnetic polarizability,
- P electric polarizability,
- X_{01} 2.405,
- X_{11}' 1.814,
- β phase factor for TE_{11} mode,
- Z_0 $\sqrt{\mu_0/\epsilon_0}$,
- ω $2\pi f_0$,
- k_0 $\omega\sqrt{\mu_0\epsilon_0}$.

For the coupling matrix of a six-pole elliptic filter with a coupling sequence specified in Fig. 1, (6) and (7) can be rewritten as follows:

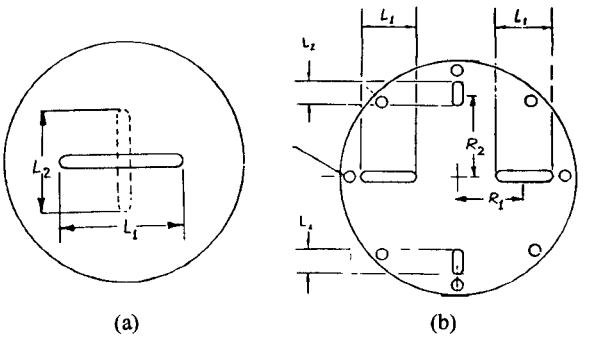

(a) (b)

Fig. 2. Intercavity aperture structure (a) as used in [6], and (b) as used in the present paper.

$$M_{16} = 2A\mu_0 M_1 J_1'^2\left(\frac{X_{11}'R_1}{a}\right) \quad (8)$$

$$M_{34} = 2A\mu_0 M_2 J_1'^2\left(\frac{X_{11}'R_2}{a}\right) \quad (9)$$

$$M_{25} = 2B\left[\frac{k_0^4}{\omega^2\epsilon_0}\left\{P_1J_0^2\left(\frac{X_{01}R_1}{a}\right)+P_2J_0^2\left(\frac{X_{01}R_2}{a}\right)\right\} + \frac{\mu_0X_{01}^2}{a^2}\left\{M_1'J_1^2\left(\frac{X_{01}R_1}{a}\right)+M_2'J_1^2\left(\frac{X_{01}R_2}{a}\right)\right\}\right] \quad (10)$$

where

$$A = \frac{\beta^2(1.841)^2}{k_0^2Z_0^2\epsilon_0\pi la^2(0.281)}\cdot\frac{f_0}{\Delta f}$$

$$B = \frac{\omega^2\epsilon_0}{J_1^2(X_{01})\pi k_0^4 la^2}\cdot\frac{f_0}{\Delta f}$$

and

- M_1, M_2 magnetic polarizability of a slot of length L_1 or L_2, respectively, with the magnetic field parallel to the length L of the slot,
- M_1', M_2' same as M_1, M_2 except the magnetic field is now parallel to the width W of the slot.
- P_1, P_2 electric polarizability of a slot of length L_1 or L_2, respectively.

By solving (8)–(10) simultaneously, it is possible to find a set of R_1, R_2, L_1, and L_2 that can satisfy all three coupling requirements.

IV. Experimental Results

A six-pole elliptic filter was realized using the aperture structure presented in Fig. 2(b). An exploded view of the mechanical configuration is shown in Fig. 3. The filter is constructed using two triple-mode cavities cascaded back-to-back. The cavities contain one coaxial coupling probe for input or output coupling, two coupling screws for intracavity couplings, and three tuning screws for independent tuning of the three orthogonal modes.

The experimental filter was synthesized to have a center frequency of 3.93 GHz with a bandwidth of 32 MHz.

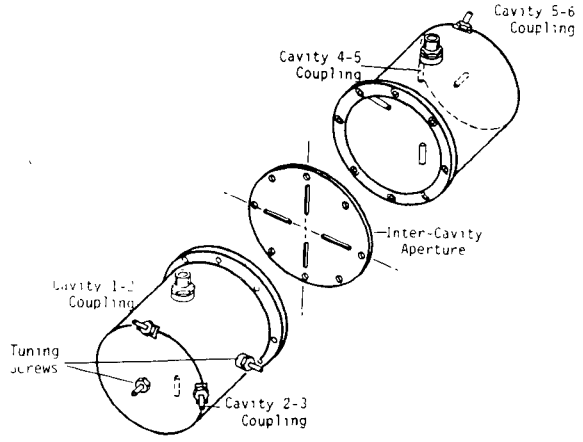

Fig. 3. Schematic diagram of the two-cavity six-pole elliptic filter.

Other specifications of this filter were: notch level = 40 dB, VSWR = 1 : 1.15. The final filter response was optimized by tuning of the filter cavities and trimming of aperture dimensions using some judicious trial and error methods.

The measured return loss of this filter is shown in Fig. 4(a). From an inspection of the variation of the return loss in the passband, it is clear that all six modes have been controlled and excited properly. The passband insertion loss of the filter is shown in Fig. 4(b). The isolation characteristic given in Fig. 4(c) clearly shows the four transmission zeros in the stopband, which is a typical feature of a true elliptic-function response. The wide-band isolation characteristic of the filter in Fig. 4(d) shows the spurious response of the filter between the 3 and 5-GHz range. These are, of course, due to the propagating higher order modes.

An interesting observation made during the experiments is that the measured Q of the filter was found to be approximately 13 K. This value is much larger than the Q obtained in normal production of a six-pole dual-mode filter, which is typically around 11 K. This large difference in Q is attributed to the fact that, in a sixth-order triple-mode filter, only one intercavity aperture, as opposed to two in a dual-mode filter, is required.

Based on the measured electrical characteristics shown in Fig. 4, a theoretical coupling matrix was synthesized by an iterative computer routine [11]. This routine calculates the element values in the coupling matrix of Fig. 1(a) such that it gives the same filter response as the experimentally measured data. The values of M_{16}, M_{34}, and M_{25} thus obtained (labeled theoretical value) can be compared with those obtained (labeled calculated value) from (8)–(10) using the experimental aperture dimensions. This comparison, presented in Table I, is useful in analyzing the errors involved in the approximate formulas (8)–(10). The first set of calculated values in Table I is obtained by assuming that the electric/magnetic fields are uniform across the aperture and are equal to the respective field at the center of gravity of the aperture. This is valid only when the aperture is small, which is not the case in general for the structure of interest here. Thus, in order to improve the accuracy, in (8)–(10) the field intensities, averaged over

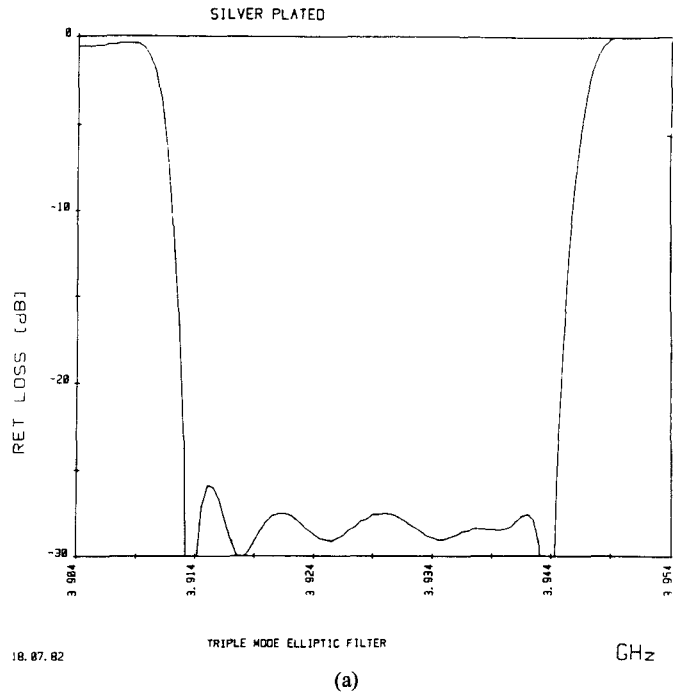

(a)

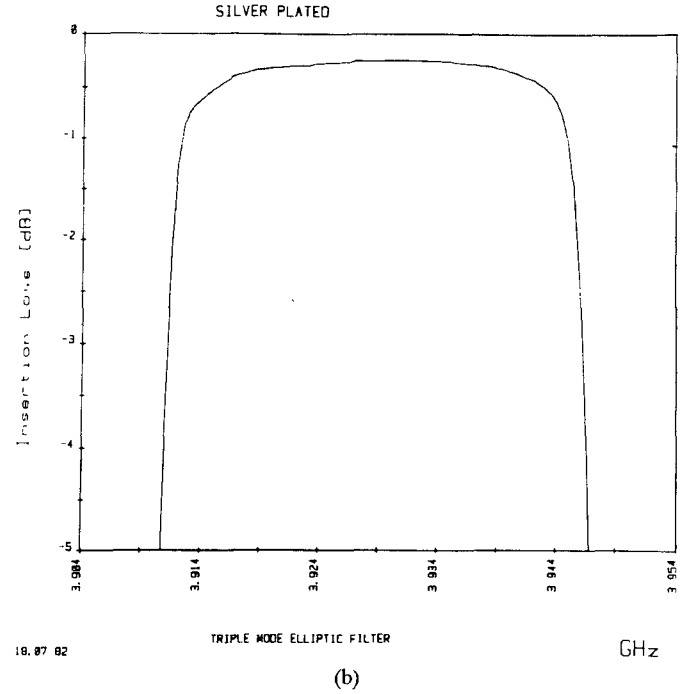

(b)

Fig. 4. (a) Measured return loss of the filter, (b) measured passband insertion loss of the filter, (c) measured isolation characteristic of the filter, and (d) spurious response of the filter between 3 and 5 GHz.

the aperture, are used. These modified results are also shown in Table I.

From the data presented in Table I, the following two observations can be made: First, there is a general reduction in the calculation errors if the field averaging over the aperture surface is used. Second, the improvement is inversely proportional to the aperture size, i.e., the larger the aperture the less significant is the improvement. Furthermore, the large discrepancy between the theoretical and the calculated values of M_{25} indicate that, besides the field intensity, other factors also contribute towards the calcu-

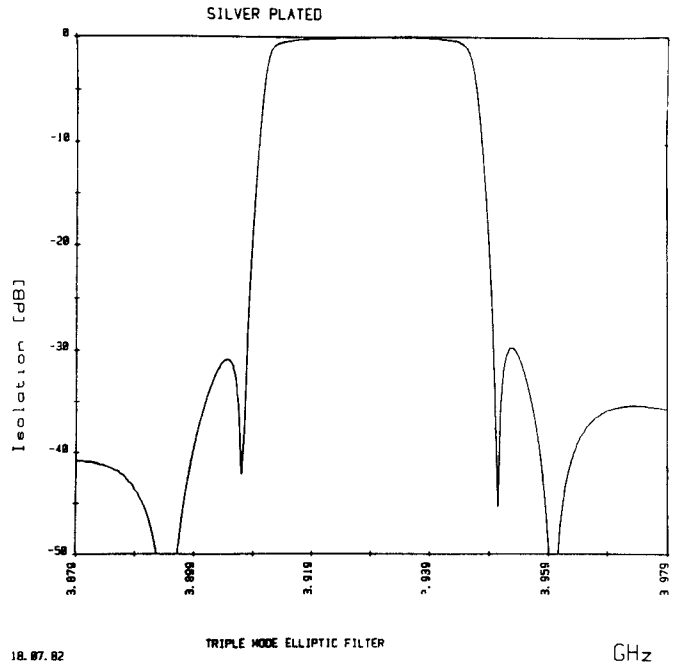

(c)

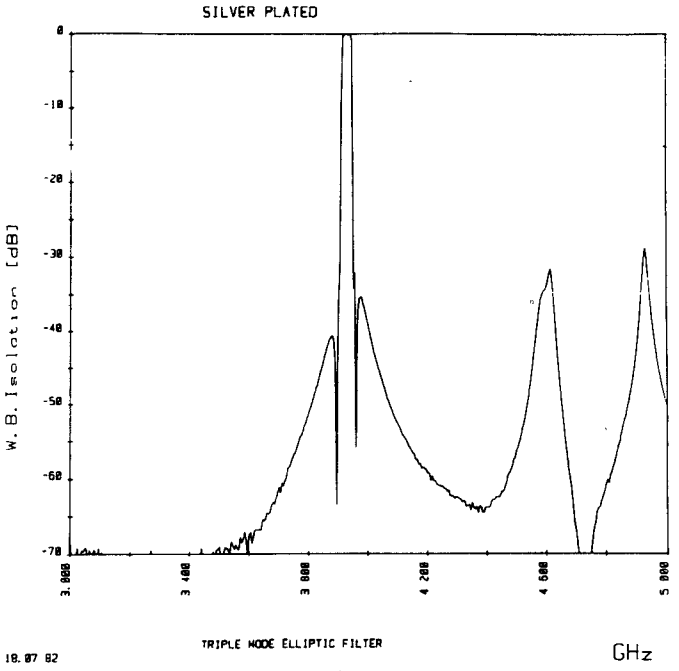

(d)

Fig. 4. Cont.

lation errors as the aperture increases in size. These factors are large aperture dimension to wavelength ratio, aperture thickness, and the values of the polarizability (P and M) used in the calculation.

In the present context, the error in the polarizability data is the most dominant reason for the discrepancy in the values of M_{25} in Table I. The polarizability data in this paper were obtained by interpolating the experimental-electrolytic-tank method results published by Cohn [12]. These measurements covered a range of aperture sizes and are tabulated in terms of width/length ratio $(W/L) \leqslant 1$, where the length is defined as the side that is parallel to the aperture magnetic field. Thus, by using a suitable curve-fitting technique, one can interpolate these data between the range $W/L = 0$ to $W/L = 1$. The rms error introduced by the interpolation is small for $W/L \leqslant 1$ [11].

TABLE I
COMPARISON OF THE THEORETICALLY SYNTHESIZED COUPLING COEFFICIENTS WITH THE FIELD-AVERAGED CALCULATIONS

Coupling	Theoretical Value	Calculated Value (without field averaging)	Calculated Value (with field averaging)
M_{16}	0.06414	0.04352	0.05684
M_{34}	0.8213	0.5136	0.5904
M_{25}	0.3136	0.0664	0.0751

For the aperture structure of Fig. 2(b), the TM-mode magnetic field is parallel to the narrow side of the slots. This arrangement makes the W/L ratio much greater than one. The method used to calculate the magnetic polarizability for this case was to use the earlier interpolation equations [11], [12] and extrapolate the data to the region $W/L > 1$. This extrapolation introduces large errors. Unfortunately, this is the best approximation available to the authors at this point.

V. Conclusions

By using a new intercavity aperture structure and proper mode sequencing, a six-pole, triple-mode, true elliptic-function response filter has been realized. The experimental results have indicated that an excellent control of the degenerate mode excitation and intercavity mode coupling is possible. In addition to the reduction in size and weight, this filter provides a much larger Q than the corresponding dual-mode counter part.

Acknowledgment

The authors wish to express their appreciation to Com Dev. Ltd., Cambridge, Ont., Canada, for use of their facilities during fabrication and testing of the filters.

References

[1] A. E. Williams, "A four-cavity elliptic waveguide filter," *IEEE Trans. Microwave Theory Tech.*, vol. MTT-18, pp. 1109–1114, Dec. 1970.

[2] A. E. Atia and A. E. Williams, "Narrow bandpass waveguide filters," *IEEE Trans. Microwave Theory Tech.*, vol. MTT-20, pp. 258–265, Apr. 1972.

[3] W. G. Lin, "Microwave filters employing a single cavity excited in more than one mode," *J. Appl. Phys.*, vol. 22, pp. 989–1001, Aug. 1951.

[4] B. L. Blachier and A. R. Champeau, "Plural-cavity bandpass waveguide filter," U.S. patent 3 697 898, Oct. 10, 1972.

[5] S. B. Cohn, "Direct-couple-resonator filters," *Proc. IRE*, vol. 45, pp. 187–197, Feb. 1957.

[6] A. E. Atia and A. E. Williams, "New types of waveguide bandpass filters for satellite transponders," *COMSAT Tech. Rev.*, vol. 1, pp. 21–42, Fall 1971.

[7] J. D. Rhodes, "The design and synthesis of a class of microwave bandpass linear phase filters," *IEEE Trans. Microwave Theory Tech.*, vol. MTT-18, pp. 189–204, Apr. 1969.

[8] R. Levy, "Filter with single transmission zeros at real or imaginary frequencies," *IEEE Trans. Microwave Theory Tech.*, vol. MTT-24, pp. 172–181, Apr. 1969.

[9] G. L. Matthaei, L. Young, and E. M. T. Jones, *Microwave Filters, Impedance-Matching Networks, and Coupling Structures*. New York: McGraw Hill, 1964.

[10] C. M. Kudsia, "A generalized approach to the design and optimization of symmetrical microwave filters for communication systems," Ph.D. dissertation, Concordia Univer., Montreal, Canada, Nov. 1978.
[11] W. C. Tang, "A triple-mode six-pole elliptic function filter," M.A.Sc. Thesis, Faculty of Graduate Studies, Univer. Waterloo, Waterloo, Ont., Canada, Aug. 1983.
[12] S. B. Cohn, "Determination of aperture parameters by electrolytic-tank measurements," *Proc. IRE*, vol. 39, pp. 1416–1421, Nov. 1951.

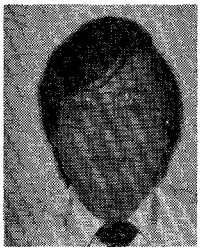

Wai-Cheung Tang (S'80–M'82) was born in Hong Kong, on November 20, 1953. He received the B.Sc. and M.Sc. degrees in electrical engineering from the University of Waterloo, Ont., Canada, in 1980 and 1983, respectively.

In 1980, he joined Com Dev. in Canada as a Microwave Engineer, where he is engaged in research and development on various types of filters and multiplexers for commercial satellite application. He is presently an Engineer Manager at Com Dev.

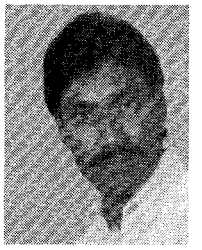

Sujeet K. Chaudhuri (M'79) was born in Calcutta, India, on Aug. 25, 1949. He received the B.E. (honors) degree in electronics engineering from the Birla Institute of Technology and Science, India, and the M. Tech. degree in electrical communication engineering from the Indian Institute of Technology, New Delhi, India, in 1970 and 1972, respectively. At the University of Manitoba Winnepeg, Man., Canada, he earned the M.Sc. degree in microwave engineering and the Ph.D. degree in electromagnetic theory in 1973 and 1977, respectively.

In 1977, he joined the University of Waterloo, Waterloo, Ont., Canada, where he is currently an Associate Professor in the Electrical Engineering Department. He has held Visiting Associate Professor's position in the University of Illinois, Chicago, during the years of 1981 and 1984. He has been involved in contractual research and consulting work with several Canadian industries and government research organizations. His current research interests are in electromagnetic scattering and diffraction with identification and imaging applications, impulse radar, and microwave components and integrated circuits.

Dr. Chaudhuri is a member of URSI Commission B, and Sigma Xi.

Accurate Hybrid-Mode Analysis of Various Finline Configurations Including Multilayered Dielectrics, Finite Metallization Thickness, and Substrate Holding Grooves

RÜDIGER VAHLDIECK

Abstract —**An accurate analysis of various finline configurations is introduced. The method of field expansion into suitable eigenmodes used considers the effects of finite metallization thickness as well as waveguide wall grooves to fix the substrate. Especially for millimeter-wave range applications, the propagation constant of the fundamental mode is found to be lower than by neglecting the finite thickness of metallization. For increasing groove depth in cases of asymmetrical and "isolated finline," higher order mode excitation reduces the monomode bandwidth significantly. In contrast to hitherto known calculations, this parameter only causes negligible influence on a fundamental mode if the groove depth is lower than half of the waveguide height.**

I. Introduction

MILLIMETER WAVE application of finline structures is of increasing importance for *E*-plane integrated circuit designs [1]–[5]. Real structure parameters, like finite metallization thickness, and waveguide grooves to fix the inset, considerably influence circuit behavior, especially in the higher frequency range. As for the metallization thickness, this influence has already been demonstrated by the example of low-insertion-loss finline and metal-insert filters [5], [6].

Hitherto known design theories [8], [11]–[18], however, widely neglect the influence of these parameters, and are considered, therefore, to yield appropriate finline circuit designs only for the lower frequency range. The unilateral earthed finline investigations by Beyer [19] reveal that both parameters have relatively high influence on fundamental mode behavior. In [19], the Ritz–Galerkin method is used and the continuity of the odd TE-mode field at the interfaces is applied as an example.

A comparison to the propagation constant of an idealized finline structure, given by Hofmann [9], seems to be in good agreement with [19] only when comparing finite strip thickness (70 μm) and zero groove depth or finite groove depth (0.326 mm) and zero strip thickness. It appears that this problem has not yet been solved completely as evi-

Manuscript received November 7, 1983; revised June 4, 1984.

The author was with the Microwave Department, University of Bremen, Federal Republic of Germany. He is now with the Department of Electrical Engineering, University of Ottawa, Ottawa, Ont., Canada K1N 6N5.

0018-9480/84/1100-1454$01.00 ©1984 IEEE